JOURNAL OF GEOPHYSICAL RESEARCH, VOL. 111, D16314, doi:10.1029/2005JD006907, 2006

Ensemble simulations of the decline and recovery of stratospheric ozone

John Austin[1] and R. John Wilson[1]

Received 24 November 2005; revised 27 March 2006; accepted 20 April 2006; published 30 August 2006.

[1] An ensemble of simulations of a coupled chemistry-climate model is completed for 1960–2100. The simulations are divided into two periods, 1960–2005 and 1990–2100. The modeled total ozone amount decrease throughout the atmosphere from the 1960s until about 2000–2005, depending on latitude. The Antarctic ozone hole develops rapidly in the model from about the late 1970s, in agreement with observations, but it does not disappear until about 2065, about 15 years later than previous estimates. Spring averaged ozone takes even longer to recover to 1980 values. Ozone amounts in the Antarctic are determined largely by halogen amounts. In contrast, in the Arctic, ozone recovers to 1980 values about 25–35 years earlier, depending on the recovery criterion adopted. By the end of the 21st century, the climate change associated with greenhouse gas changes gives rise to a significant superrecovery of ozone in the Arctic but a less marked recovery in the Antarctic. For both polar regions, ensemble and interannual variability is greater in the future than in the past, and hence the timing of the full recovery of polar ozone is very sensitive to the definition of recovery. It is suggested that the range of recovery rates between the hemispheres simulated in the model is related to the overall increase in the strength of the Brewer-Dobson circulation, driven by increases in greenhouse gas concentrations.

Citation: Austin, J., and R. J. Wilson (2006), Ensemble simulations of the decline and recovery of stratospheric ozone, *J. Geophys. Res.*, *111*, D16314, doi:10.1029/2005JD006907.

1. Introduction

[2] The timing of future ozone recovery remains an important topic [e.g., *World Meteorological Organization* (*WMO*)/*United Nations Environment Programme* (*UNEP*), 2003; *Newchurch et al.*, 2003; *Steinbrecht et al.*, 2006; *Yang et al.*, 2006; *Miller et al.*, 2006], driven by scientific questions such as: Will the Antarctic ozone hole recover and if so when?, Is a similar hole likely to form over the Arctic?, Will Arctic ozone decrease any further?, What are the influences of ozone change on the troposphere?, How is the Greenhouse effect influenced by future ozone recovery? The questions have become increasingly sophisticated over the years and now demand the use of coupled chemistry-climate models for their answer. These models have all the problems associated with climate models such as the need to have appropriate control runs and, to some degree, the need to carry out ensemble simulations, to ensure that model changes are a result of the changes in external parameters rather than internal model variability.

[3] Many processes affect atmospheric ozone concentrations. The direct chemical effect is via HO_x, NO_x, ClO_x and BrO_x reactions [e.g., *Brasseur and Solomon*, 1987]. Hence any process controlling the radical source molecules H_2O, N_2O, chlorofuorocarbons (CFCs) and halons is important. Ozone chemistry is temperature-dependent, so changes in concentrations of the well-mixed greenhouse gases (GHGs) are also significant, particularly CO_2 in the stratosphere. Hereafter we refer to GHGs as implying just the well-mixed greenhouse gases. Ozone itself and the source molecules are transport-dependent and hence any process affecting transport and its future change [e.g., *Butchart and Scaife*, 2001; *Butchart et al.*, 2006] is likely to play a role in slowing or accelerating ozone depletion. Ozone is a radiatively active gas which tends to give rise to negative feedback. For example decreasing temperatures typically slows ozone catalytic destruction cycles which increases ozone leading to more solar heating. However, in the presence of polar stratospheric clouds (PSCs) reducing temperatures in the presence of large halogen amounts leads to increased ozone depletion [e.g. *Austin et al.*, 1992]. There are also considerable uncertainties in the trends in water vapor [*Randel et al.*, 2004] and models are typically unable to simulate the past evolution in concentrations. As well as having an impact on ozone in the gas phase, via HO_x catalyzed destruction, the concentration of water vapor affects the distribution of PSCs. It is perhaps not surprising that when all these coupling processes have been included in models, a wide range of results has been produced, particularly for the polar regions where dynamical variability is large [*WMO*, 2003, chapter 3; *Austin et al.*, 2003].

[4] In this work, results from a new model are presented to address primarily the issue of ozone recovery. There are

[1]Geophysical Fluid Dynamics Laboratory, Princeton, New Jersey, USA.

0148-0227/06/2005JD006907$09.00

Table 1. Brief Description of Model Simulations

Experiment	Description	Duration, years
SL1960	time slice 1960 conditions	30
SL2000	time slice 2000 conditions	30
TRANSA	transient 1960–2005 initialized year 10 of SL1960	45
TRANSB	transient 1960–2005 initialized year 20 of SL1960	45
TRANSC	transient 1960–2005 initialized year 30 of SL1960	45
FUTURA	transient 1990–2100 initialized year 30 of TRANSA	110
FUTURB	transient 1990–2100 initialized year 30 of TRANSB	110
FUTURC	transient 1990–2100 initialized year 30 of TRANSC	110

many definitions of ozone recovery, concentrating for example on the start of ozone recovery both using models [*Austin et al.*, 2003] and observations [*Newchurch et al.*, 2003; *Reinsel et al.*, 2005; *Yang et al.*, 2006; *Miller et al.*, 2006]. A cautious approach [*Weatherhead et al.*, 2000], takes recovery as being confirmed when a statistically significant ozone increase has been observed. Their conclusion was that at least fifteen years of observations are required before the start of ozone recovery can be confirmed. Caution concerning recovery has also been expressed by *Steinbrecht et al.* [2006], while *Steinbrecht et al.* [2004] point out the difficulty of identifying ozone recovery in the context of solar variability.

[5] In this work, we address ozone recovery from a simpler point of view. The start of recovery is determined as the date of ozone minimum in the time averaged results and the date of full recovery as the time averaged return to 1980 total ozone amounts. Attributing ozone loss to halogens, built into some of the definitions of recovery, is here considered important but different from the issue of recovery itself. Instead, 11-year running means are used to reduce the effects of the solar cycle and internal model variability. While some ozone depletion took place before 1980 [e.g., *Solomon et al.*, 2005], as also shown in the model results presented here, it is a convenient definition of the start of ozone loss, as extensive stratospheric observations have existed only since the beginning of the satellite era.

2. Model Description and Simulations Completed

[6] The Geophysical Fluid Dynamics Laboratory (GFDL) Atmospheric Model with Transport and Chemistry (AMTRAC), is described by *Austin et al.* [2006] and is a combination of the GFDL AM2 [*Anderson et al.*, 2004] with chemistry from UMETRAC [*Austin and Butchart*, 2003]. The AM2 has since been updated with finite volume advection and the chemistry has been improved principally regarding the treatment of the long-lived tracers, as described in more detail by *Austin et al.* [2006]. The chemistry module is a comprehensive stratospheric scheme with simplified tropospheric chemistry and is fully coupled to the climate model. The photolysis rates are determined from the altitude, ozone column and solar zenith angle using a precomputed look-up table. The table was constructed using the methods of *Groves and Tuck* [1980], but with updated photochemical data [*Sander et al.*, 2003] in which the solar beam is followed through the atmosphere, with explicit account taken of the geometry of the path length. Photolysis rates are calculated for solar zenith angles which exceed 90°, but no allowance is made for refraction of the solar beam.

[7] The model resolution is 2° by 2.5° with 48 levels from 0.0017 hPa to the ground. The vertical grid spacing decreases steadily from the top of the atmosphere and in the upper stratosphere is about 4 km, decreasing to 1.5 km in the lower stratosphere. The nonorographic gravity wave forcing scheme due to *Alexander and Dunkerton* [1999] is included in the model.

[8] The model simulations are shown in Table 1. Both time slice runs used sea surface temperatures and sea ice amounts (hereafter referred to jointly as SSTs) from a 1960 to 2000 climatology. The GHG concentrations were set to the values appropriate to the specific calendar year. A solar

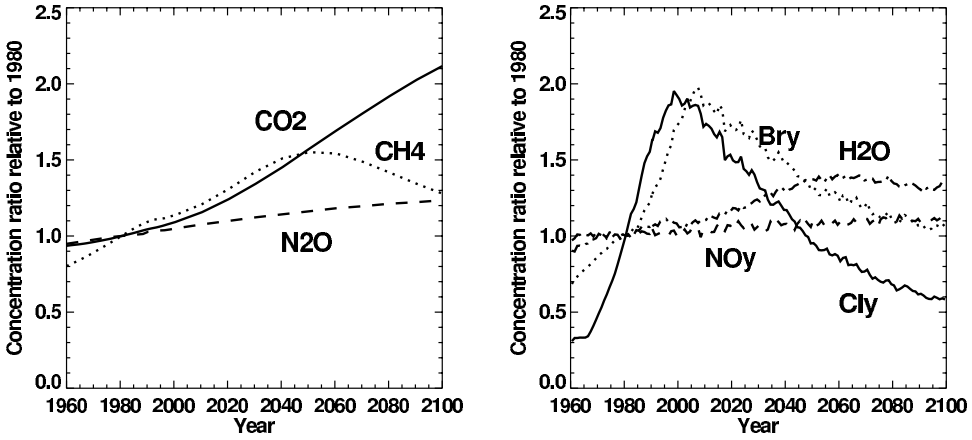

Figure 1. (left) Concentrations of the GHGs during the simulations relative to the values at 1980. The 1980 values assumed were CO_2 337.95 ppmv, CH_4 1.547 ppmv, and N_2O 301.0 ppbv. (right) Model values from simulations TRANSA and FUTURA at the equator for the long-lived families relative to the values at 1980, which were Cl_y 1.654 ppbv, Br_y 8.69 pptv, H_2O 4.31 ppmv, and NO_y 17.61 ppbv. Cl_y, Br_y, and H_2O are given at 1.3 hPa; NO_y is given at 3.6 hPa.

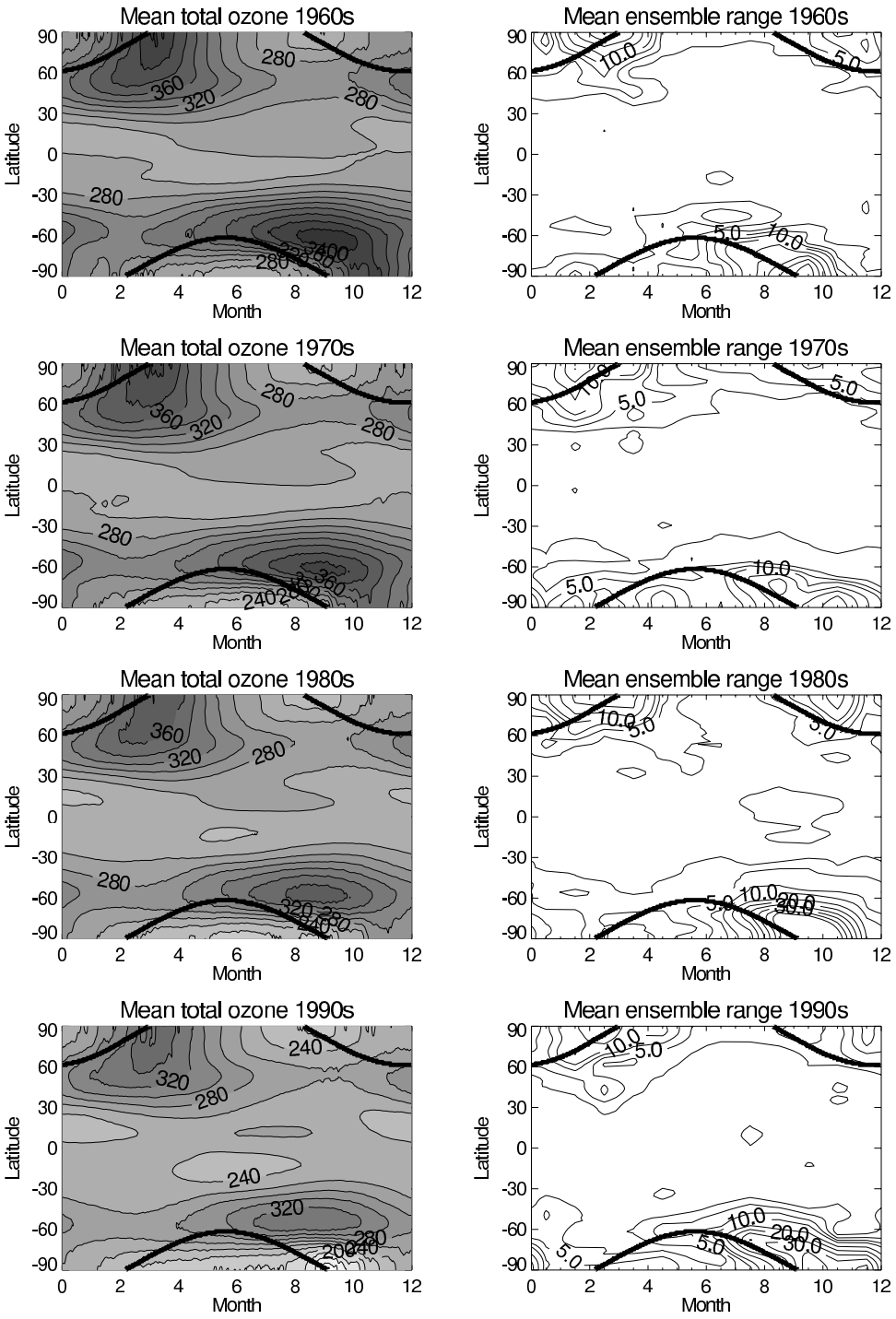

Figure 2. (left) Decadal and ensemble mean total ozone amounts for the past simulations TRANSA, TRANSB, and TRANSC as a function of latitude and month. The contour interval is 20 DU. (right) Range in the ensemble decadal means. The contour interval is 2.5 DU up to 10 DU and 5 DU thereafter. The thick black lines indicate the edge of the region observed by TOMS, approximately the position of the terminator.

cycle was not present in the forcing and aerosol amounts were set to background levels.

[9] For the past runs, the model was forced with the same time-dependent prescription of GHG and CFC concentrations, tropospheric and volcanic aerosols, and the solar cycle as from *Delworth et al.* [2006] and *Knutson et al.* [2006]. Sea surface temperatures were obtained from the Hurrell data set (J. Hurrell et al., personal communication, 2005), extended to the beginning of the year 2005. For the future runs, the Intergovernmental Panel on Climate Change (IPCC) scenario A1B [*IPCC*, 2001, Appendix II] was used for the GHGs. The rate of change of active chlorine and

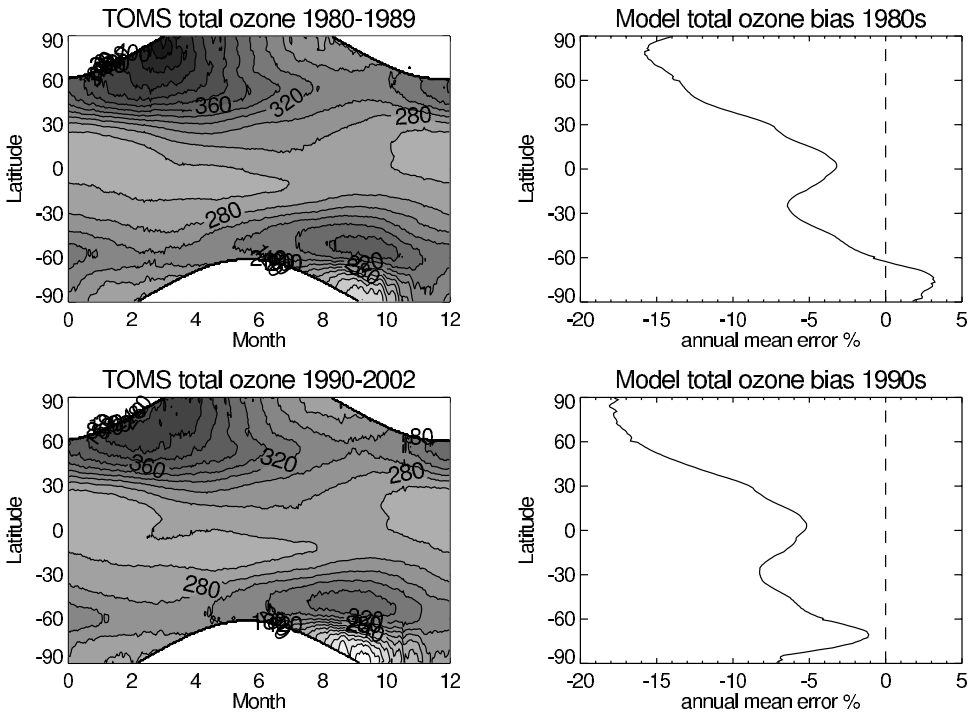

Figure 3. (left) Decadal and ensemble mean total ozone amounts from TOMS version 8 data as a function of latitude and month. The contour interval is 20 DU. Polar night is indicated by the contour-free regions. (right) Annual mean model bias (model - TOMS) in percent. For the polar regions, biases were calculated only for those days where TOMS made measurements and hence the results beyond 60° latitude are not strictly an annual mean.

bromine amounts in the model are computed using empirical functions of the destruction rates for each significant CFC and halon. CFC and halon concentrations were taken from *WMO* [2003, chapter 1, reference profile A1]. However, because of model underprediction of age of air in comparison with measurements found in previous simulations of the model, it was found to be necessary to enhance the effective destruction rates of the CFCs by 25% to obtain more accurate Cl_y concentrations. The Br_y values were not corrected, since the age of air underprediction was found not to have a significant impact.

[10] Volcanic aerosol amounts were taken as background values and constant for the future. The optical depths were averaged from observations over the period 1996 to 1998 and the results were smoothly joined to the data from 1997 onward. This results in higher aerosol values than observed for the period 1997 to 2005. At these concentrations, the influence of aerosol changes on the results is small but, arguably, the values are more representative of a post volcanic atmosphere over the long term than, for example, the current very clean stratosphere. Sea surface temperatures and sea ice amounts were taken from a coupled atmosphere-ocean model simulation of the same core climate model, but with fewer vertical levels (simulation CM2.1 of *Delworth et al.* [2006]). A solar cycle was maintained into the future by repeating the last 5 cycles for which detailed observations of 10.7 cm radio flux are available.

[11] The past runs were initialized from years 10, 20 and 30 of the 1960 time slice run. Unfortunately, because of different aerosol amounts and difference in the amount of solar forcing, the past runs still needed a few years to spin up to their balanced state. The future runs were initialized from 1 January 1990 of the corresponding past run. A fifteen year overlap between the past and future runs was set up to test the impact of the switch in sea surface temperatures from observation to model results. In most cases this had no impact on the model results.

3. Greenhouse Gas Concentrations and Long-Lived Species

[12] The main long-lived species which affect ozone are shown in Figure 1. In Figure 1 (left) are shown the GHGs for the troposphere, which were specified. In Figure 1 (right), values are shown for long-lived chemical species computed by the model near the equatorial stratopause. All the values have been scaled to the values for 1980 (see Figure 1 caption for details). The CO_2 and N_2O amounts are taken to increase steadily. Methane amounts are taken to increase in the early part of the integration and are taken to decrease from about 2050. The methane amounts, together with changes in the tropical tropopause temperature, give rise to the changes in water vapor amounts shown in Figure 1 (right). By 2060, water vapor amounts had increased by about 40% but did not decrease substantially in the final few decades despite lowering methane amounts.

[13] The Cl_y and Br_y concentrations at 1.3 hPa at the equator are shown in Figure 1 (right) throughout the 140-year simulation period. At this location, modeled Cl_y peaked at 3.3 ppbv in 1997 and Br_y peaked at 17.2 pptv in 2007. Return to 1980 values is projected to occur by about

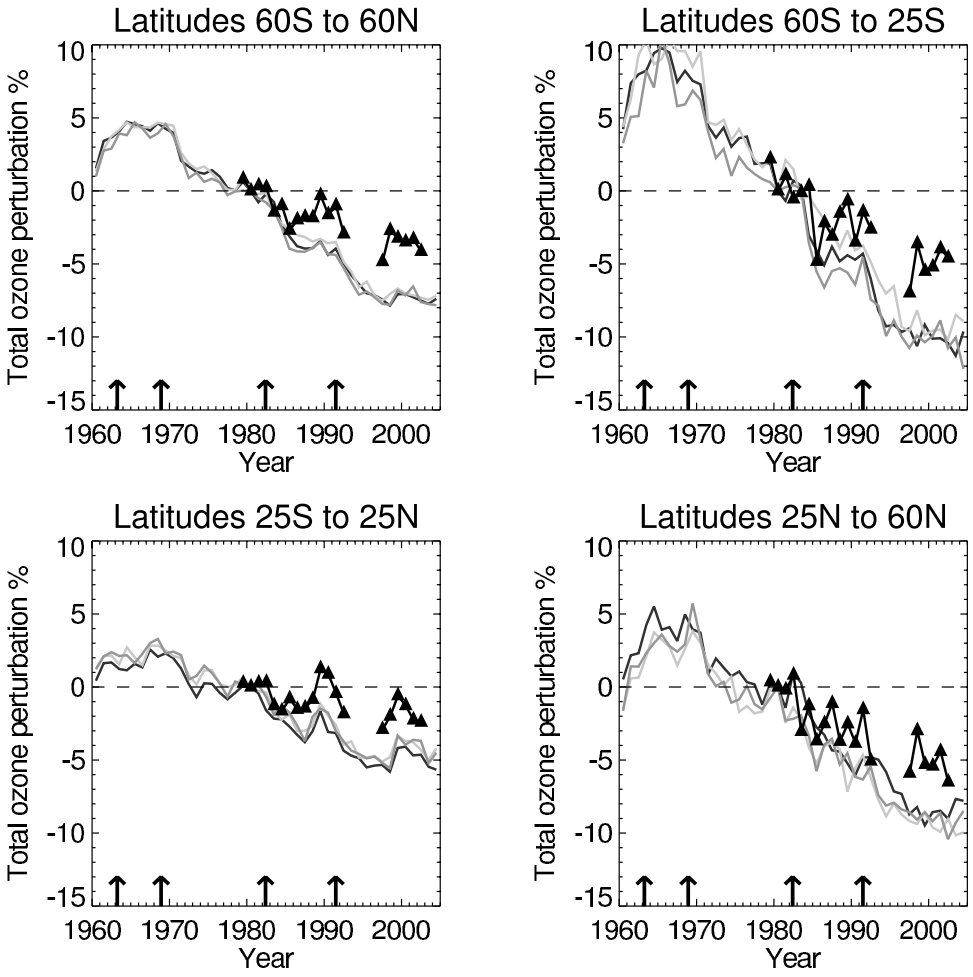

Figure 4. Annually averaged total ozone for the three simulations for selected latitude ranges (solid lines). The values plotted are perturbations in percent from the 1980 values. The results for TOMS version 8 are shown by the black lines with triangles. The dates of the volcanic eruptions of Agung (1963), Fernandina (1968), El Chichon (1982) and Pinatubo (1991) are indicated by the arrows on the abscissa.

2050 for Cl_y but not before the end of the simulations for Br_y. The amount of NO_y at 3.6 hPa at the equator, near the model peak, increased only slightly during the simulations.

4. Past Simulations of Ozone

4.1. Decadal Variation in Total Ozone

[14] Figure 2 (left) shows the decadal averages of simulated total ozone averaged over all three ensemble members. Tropical ozone decreased throughout the period from about 260 DU in the 1960s to below 240 DU by the 1990s. In the Northern Hemisphere, maximum ozone occurred over the North Pole in spring time with a distinct minimum over the Arctic during autumn. In the Southern Hemisphere, peak ozone values occurred in middle to high latitudes, with the Antarctic ozone hole occurring in the 1980s and 1990s. Ozone decreased everywhere during the simulations.

[15] Figure 2 (right) shows the range in the ensemble members. Data from each of the simulations was averaged over decade and over days in the month before calculating the range. There was considerable daily variability necessitating the monthly averaging before calculating the range in order to observe a clear signal. In the tropics and subtropics, the ensemble range is small, typically less than 2.5 DU. The range is much larger in the polar regions and exceeds 30DU over the South Pole in the later decades. This demonstrates the well-known behavior [e.g., *WMO*, 2003, chapter 3] that largest atmospheric variability and uncertainty occurs in the polar regions.

[16] Decadal averages from Total Ozone Mapping Spectrometer (TOMS) version 8 data [*Wellemeyer et al.*, 2004; P. K. Bhartia and C. G. Wellemeyer, TOMS-V8 total O3 algorithm, available at http://toms.gsfc.nasa.gov/version8/version8_update.html, document toms_atbd.pdf, 2005) and model biases are shown in Figure 3. The TOMS data, nominally for the 1990s, here includes also the years 2000–2002 to compensate for the gaps in data coverage during 1993 to 1996. The model seasonal variations (Figure 2) are in good agreement with TOMS, and hence, for clarity, Figure 3 (right) shows only the annual mean model bias. For both decades, the latitudinal variation of the bias is very similar but with larger biases in the 1990s. In the Southern Hemisphere, the results are in good agreement with observations in both decades, with biases typically about 5%

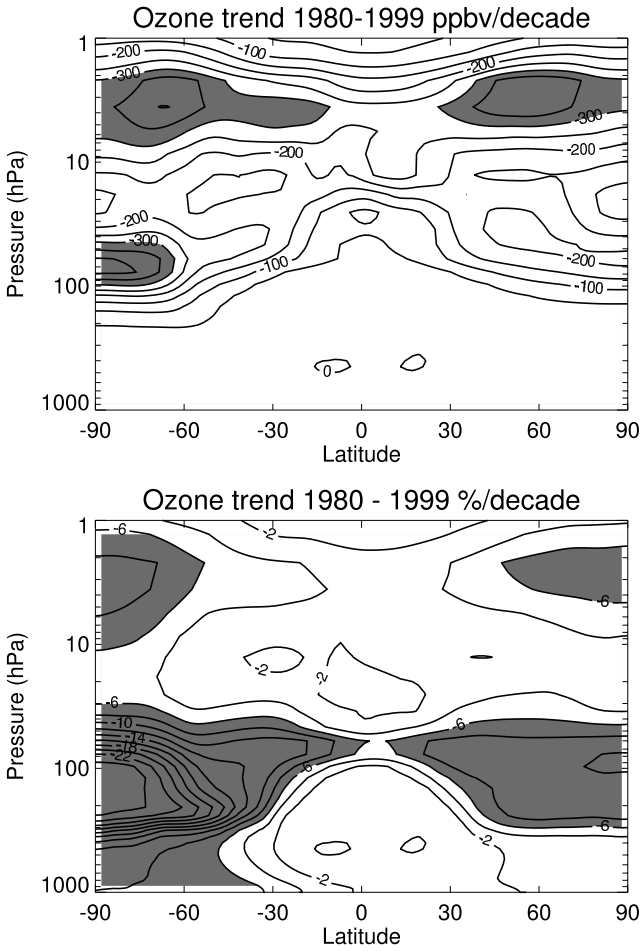

Figure 5. Annually averaged ozone trends for the period January 1980 to December 1999 as a function of latitude and pressure, averaged for the three ensemble members. Decreases exceeding (top) 300 ppbv per decade and (bottom) 6% per decade are indicated by the shading. Trends larger than about 1.5% per decade (4% in the lower stratosphere poleward of 75°) are statistically different from zero at the 95% confidence level.

in magnitude. The model's low bias increases steadily with latitude toward the North Pole, where it reaches about 15%.

4.2. Regionally Averaged Total Ozone

[17] Area averaged ozone for tropical and midlatitudes is shown in Figure 4 in comparison with TOMS version 8 data. TOMS (version 7) and ground-based data show similar trends [*Fioletov et al.*, 2002]. Over the period 1980–2000, the general pattern of the observations was reproduced, but the simulated ozone decreased by about 2% per decade globally relative to the observations. The impact of the eruptions of El Chichon and Mount Pinatubo are particularly apparent in the observed tropical values, resulting in a decrease of about 2% for El Chichon (May 1982) and more than 3% for Mount Pinatubo (June 1991), relative to the preeruption date. The model reproduced these features, but they are partially obscured by the overall model trend. During the eruption of Agung (March 1963) and Fernandina (November 1968), model ozone values increased in accordance with the study of *Tie and Brasseur* [1995]. During the 1960s the impact of the heterogeneous reactions on the volcanic aerosol was to convert N_2O_5 to HNO_3 which reduces catalytic ozone destruction by NO_x. This mechanism is later superseded by halogen effects for which catalytic ozone destruction is increased by heterogeneous reactions. In comparison, *Dameris et al.* [2005] and C. Brühl et al. (personal communication, 2005), obtain results which agree better with observations for the recent past, and show a smaller ozone increase from the Agung eruption. In that case the stratospheric temperature increase following the eruption was much larger than in AMTRAC and any reduction in NO_x catalyzed destruction was counterbalanced by increased HO_x catalyzed destruction.

[18] Ozone trends were computed for the period 1980 to 1999 by performing a least squares fit of the annually averaged ozone values against time. The results, as a function of latitude and pressure are shown in Figure 5. The results are very similar to those obtained using a previous version of the chemical model, but a different climate model [*Austin*, 2002]. The results also agree well with observations over a broad spatial range (Figure 6). In the upper stratosphere, the ozone reduction peaked at over 8% per decade in southern high latitudes, slightly more than observed, but in northern high latitudes, the reduction rate is slightly less than observed. The development of the ozone hole is prominent between 300 and 40 hPa and a similar large loss of up to 10% per decade occurred in the model Arctic compared with 5% per decade observed. Typically, trends exceeding about 1.5% per decade in the model, increasing to 4% per decade in the polar lower stratosphere are statistically different from zero.

[19] In the model results, ozone decreased everywhere, whereas in the observations there is additionally a band in the tropical middle stratosphere where the ozone increased slightly. This increase is not statistically significant. In general, although there are quantitative differences between observations and model, the model results show similar qualitative behavior as the observations, with less ozone depletion in the middle stratosphere than in the upper and lower stratosphere. In the troposphere, the observed trends

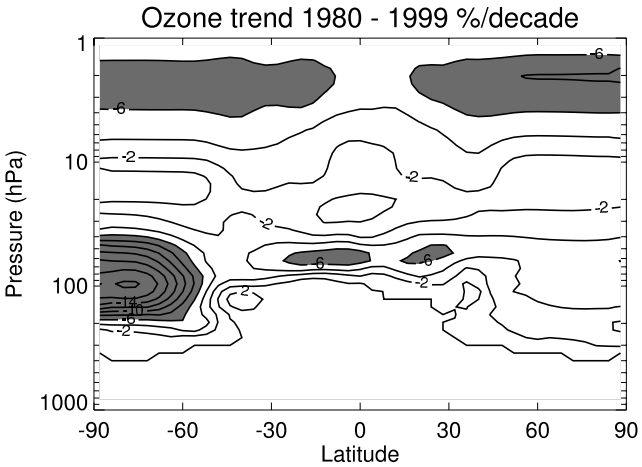

Figure 6. Observed annually averaged ozone trends for the period January 1980 to December 1999 as a function of latitude and pressure, taken from a variety of in situ and satellite data (W. Randel, personal communication, 2005).

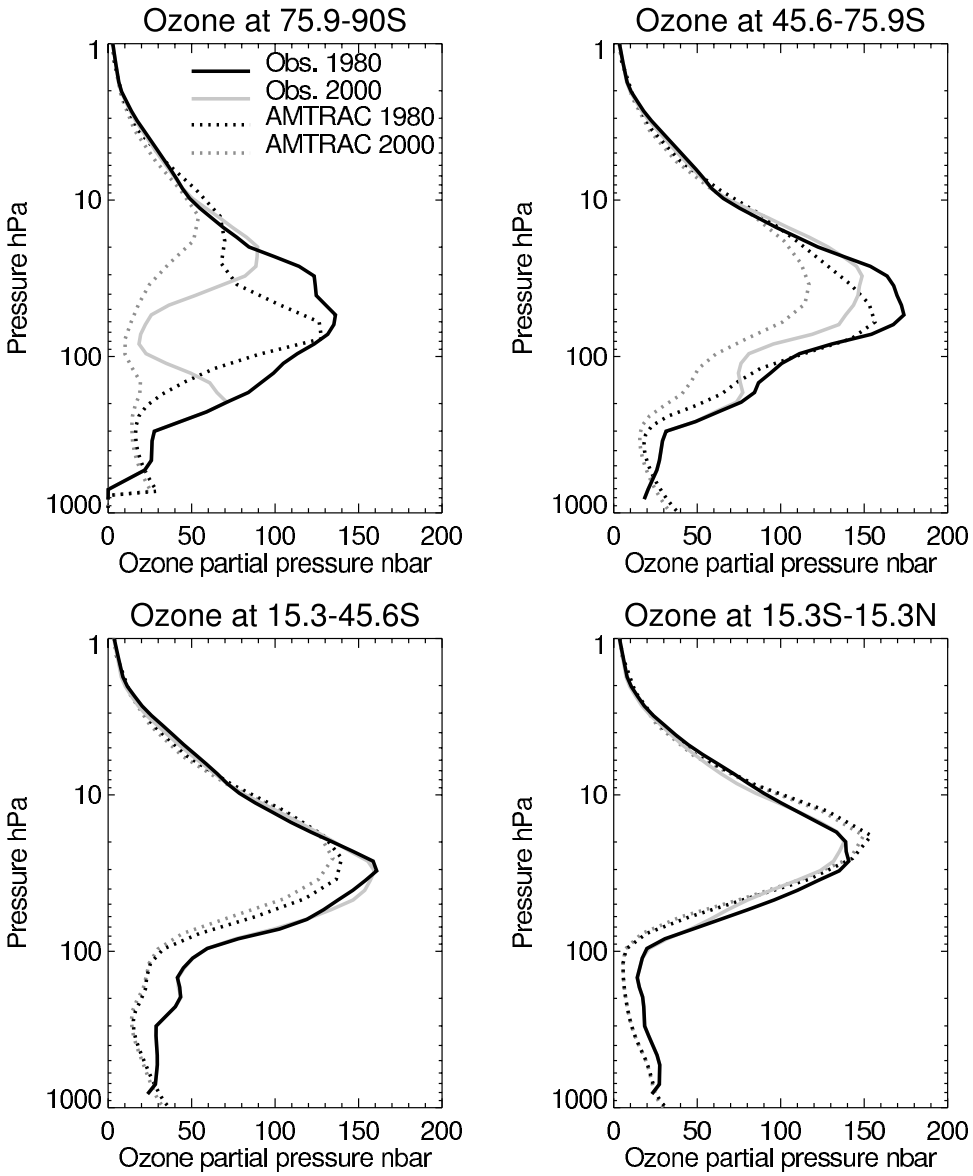

Figure 7. Selected vertical profiles of monthly mean ozone partial pressure for October simulated by the model (TRANSA) and compared with observations (W. Randel, personal communication, 2005) averaged over the indicated latitude bands. Solid lines indicate observations; dotted lines indicate model results. Lines for the year 2000 are in gray; lines for the year 1980 are in black.

are not significantly different from zero, but simulated ozone decreased by several percent per decade. In the model the results are influenced by downward transport from the ozone hole and increased HO_x depletion arising from increased water vapor. The former could be due to numerical mixing, arising from the limited resolution in the vicinity of the tropopause. Increases in NO_x would increase ozone in the troposphere and correct the model error, but in the model simulations NO_x has been kept constant there.

4.3. Vertical Profiles of Ozone

[20] Figures 7 and 8 compare vertical profiles of ozone for 1980 and 2000 with observations in the spring season (October and March averages) over latitude ranges representing the tropics, subtropics, midlatitudes and polar regions. Similar results are obtained for other years near 1980 and 2000, respectively. The results are expressed as a partial pressure so that areas between the curve and the ordinate over a given pressure range are proportional to the ozone column between those levels. Figure 7 shows that the development of the ozone hole at the pole is more prominent and deeper than observed in 2000. Model ozone reductions between 1980 and 2000 were also larger than observed in middle and high latitudes.

[21] In the subtropics and tropics, the model agrees better with observations throughout the pressure range. Nonetheless, the model tended to underpredict ozone in the upper troposphere and lower stratosphere. This was compensated in part by higher modeled ozone amounts in the middle and upper stratosphere. A similar level of agreement was

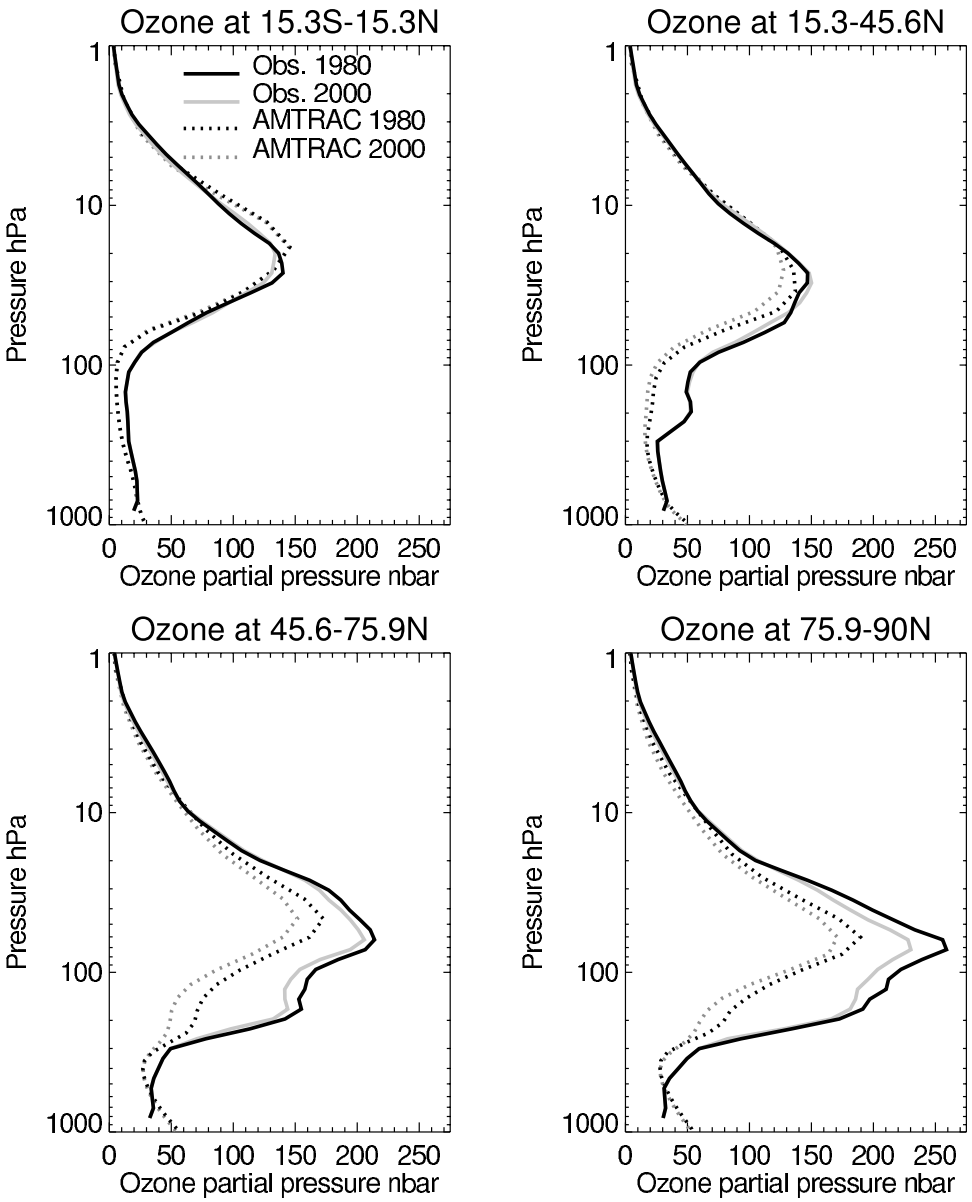

Figure 8. As Figure 7, but for the Northern Hemisphere for March.

obtained with observations in the Northern Hemisphere, except that the model substantially underpredicted observations in the range 20 to 200 hPa in middle and high latitudes. There was also a clear reduction in ozone over the period 1980 to 2000 throughout the pressure range 20 to 200 hPa.

4.4. Global Ozone Comparison for the Recent Past

[22] Figure 9 compares globally averaged ozone from the ensemble member "A," runs TRANSA and FUTURA, during the 15-year overlap period 1990–2005. The two simulations agree within about 2 DU throughout the period, indicating that there is no overall systematic difference between the two sets of simulations. The other ensemble members showed similar results. Absolute ozone amounts for TRANSA and FUTURA were about 5 DU higher than the time slice run SL2000 because of different sea surface temperatures (SSTs), solar cycle and aerosol amounts, which were fixed in run SL2000 but varying as observed in the other runs.

5. Future Simulations of Ozone

[23] While there are some discrepancies between model results and observations, as indicated in sections 4.1 to 4.3, apart from a 2%/decade trend bias, there is overall general agreement with absolute values and trends over the last 20 years. Thus it is suggested that the model can be used to provide a useful indication of future stratospheric change. The results of section 4.4 (and other diagnostics examined but not shown) concerning the period of overlap between the past and future simulations suggest also that the simulations may be joined to form a continuous time series of results, without significant loss of accuracy.

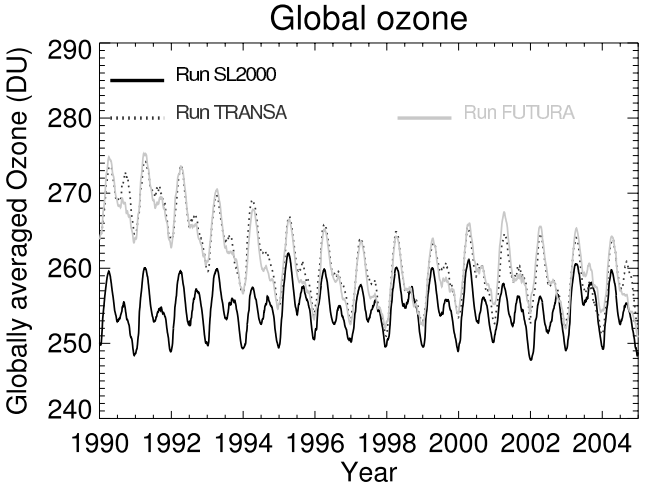

Figure 9. Globally averaged total ozone for the simulations TRANSA and FUTURA in comparison with the results from run SL2000, for the 15-year overlap between the experiments.

5.1. Decadally Averaged Ozone

[24] Figure 10 shows the variation of total ozone averaged over selected decades as a function of latitude and day of the year (compare with Figure 2). Results are presented every 3 decades, and the results evolved steadily in the intermediate decades. Minimum ozone occurred in the model results in the decade 2000–2010 and ozone increased steadily thereafter. The seasonal ozone variation is very similar in the entire set of simulations, with a maximum in the Arctic spring at the pole and a minimum in the tropics and in the Arctic autumn. In the Southern Hemisphere, the midlatitude ozone maximum was prominent throughout the simulation and the ozone hole gradually subsided from its peak in the 2000–2010 decade. A small ozone hole was still present in the decade 2060–2070, as discussed in section 5.2.

5.2. Low and Midlatitude Total Ozone

[25] Figure 11 shows the regionally averaged total ozone for the full time span of the experiments, expressed as a perturbation from the 1980 values (compare Figure 4). As in the case of global ozone, there is very little systematic difference between the experiments during the overlap years as indicated by the barely noticeable increase in the spread of the plotted results during the 1990 to 2005 period. All four latitude ranges show similar results indicating a minimum in the ozone perturbation at about 2000–2005, and recovery thereafter. Recovery of ozone to 1980 values occurs by about 2040, depending on the latitude, as discussed in more detail in section 6. For the near global average (Figure 11, top left), regular oscillations are present, with peak to peak values of about 3% due to the 11-year solar cycle. This is consistent with results obtained [*Labitzke et al.*, 2002] with the previous version of the model chemistry and with other models and observations [*Shindell et al.*, 1999]. In common with those models, the change in ozone column due to the solar cycle agrees reasonably well with observations, but during solar maximum, ozone is overpredicted in the middle stratosphere and underpredicted in the upper stratosphere (see Shindell et al., Figure 3).

5.3. Polar Ozone

[26] The evolution of minimum spring ozone for the transient simulations is shown in Figure 12 in comparison with TOMS data. The spring periods are defined as September to November (Antarctic) and March to April (Arctic), and may be compared with the results of other models presented by *Austin et al.* [2003] and *WMO* [2003, Figures 3–46 and 3–47]. The model is biased low by about 30–45 DU over Antarctica, but because of the rapid development of the ozone hole, this does not become apparent until the minimum is attained at about the year 2000. The results are compared on the same graph with the halogen amount, $Cl_y + 50 \times Br_y$, using the chemical concentrations at 35 hPa for the respective polar point. *WMO* [2003, section 1.4.4] discusses different ratios for the impact of Br_y on ozone relative to the Cl_y impact. Values between 45 and 60 are discussed, but here we use a value of 50, although the results obtained are not sensitive to the precise value chosen.

[27] The ozone hole may be considered to have begun in the model when the minimum column dropped below 175 DU, indicated by the broken line parallel to the abscissa of Figure 12. Rapid ozone loss occurred during the period 1980 to 2000. Minimum column ozone was linearly related to halogen amount to a very good approximation suggesting the dominance of chemical processes rather than climate or water vapor related issues. During the slower ozone recovery phase, ensemble and interannual variability increased markedly. Hence the timing of full recovery in the model is very sensitive to its definition, although the timing of the formation of the ozone hole is much clearer. For example, defining an ozone hole in the model as that below 175 DU (equivalent approximately to the classical definition of 220 DU for the real atmosphere, after allowing for model bias), the Antarctic ozone hole occurs from about 1979 onward but does not disappear until about 2065 on average. Choosing 190 DU gives a formation date of just one or two years earlier, but adds 20 years to the date of full recovery.

[28] Minimum ozone in the Arctic is biased low by about 30 DU. For the past, the overall model trend is in broad agreement with observations and indicates some dependency on the halogen amount. Model ozone reached its minimum during the period 2000–2020 and then recovered. Recovery to 1980 values occurred by about 2040, but during the recovery phase, ozone was only weakly related to halogen amounts, with the difference due to interannual variability in the model dynamics. The minimum Arctic ozone in all the runs was 184 DU, or about 215 DU after correcting for the bias in the very low stratosphere, despite some 165 years of simulations in transient mode and 30 years of the 2000 time slice run, covering the period 1990–2030. In common with model results presented by *Austin et al.* [2003] and *WMO* [2003, chapter 3], there is therefore no indication in any of the simulations of an Arctic ozone hole of comparable magnitude as occurs in Antarctica.

[29] The size of the ozone hole in the simulations, defined by the area within the 220 DU contour, averaged over the period 21–30 September is shown in Figure 13 (left)

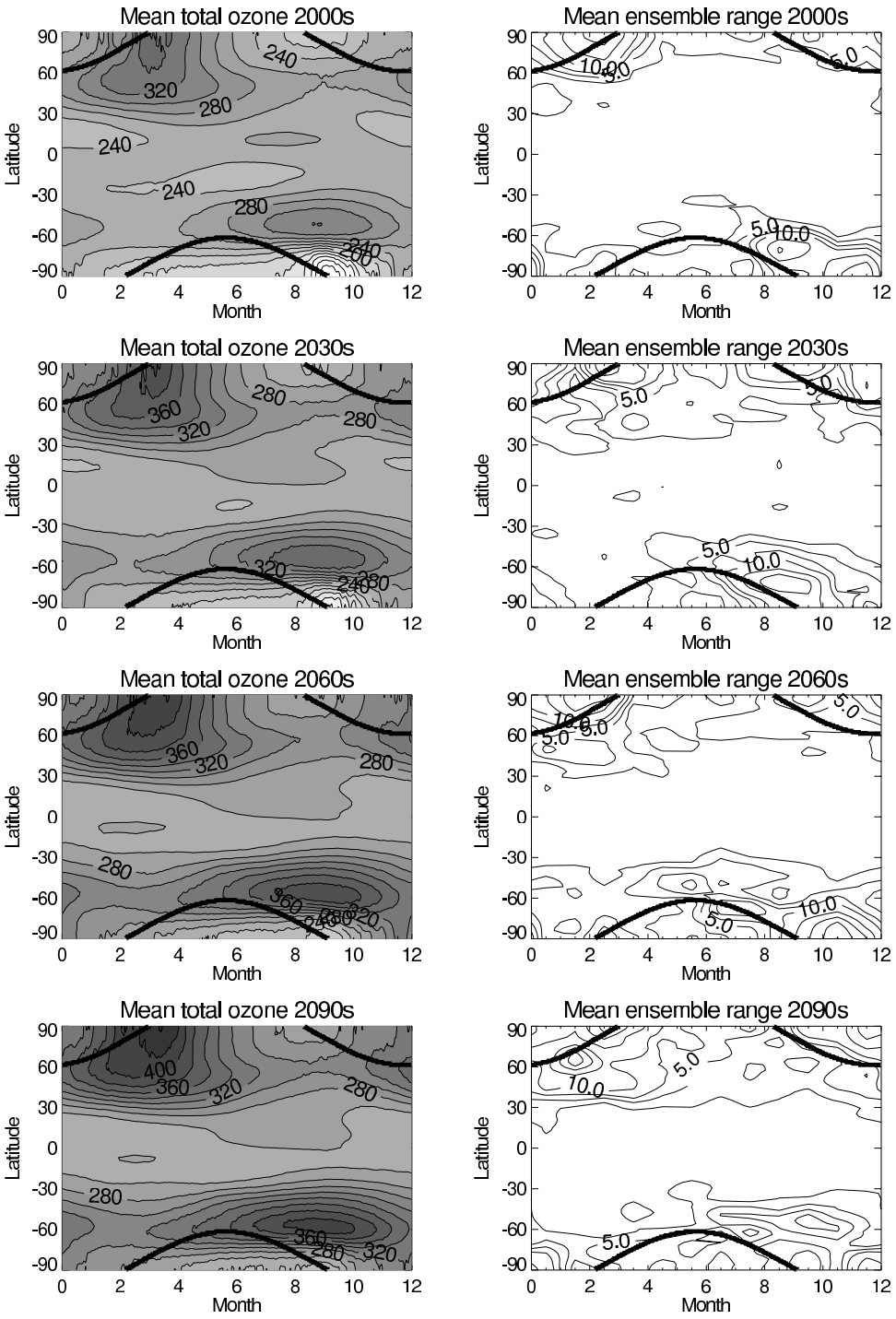

Figure 10. (left) Decadal and ensemble mean total ozone amounts for the future simulations FUTURA, FUTURB, and FUTURC as a function of latitude and month. The contour interval is 20 DU. (right) Range in the ensemble decadal means. The contour interval is 2.5 DU up to 10 DU and 5 DU thereafter. The thick black lines indicate the edge of the region observed by TOMS, approximately the position of the terminator.

together with observations from TOMS version 8 data [*Newman et al.*, 2006]. This period corresponds approximately to when the area typically reaches its maximum size in the observations. The model results are in good agreement with observations, but the model low bias seen in Figure 12 has a significant effect on the results. In view of this bias, more appropriate results are shown in Figure 13 (right), which compares the observed areas for 220 DU and the model results for 175 DU, indicating that the model ozone hole is effectively too small.

[30] In general the results are a considerable improvement on many results of *Austin et al.* [2003]. These improve-

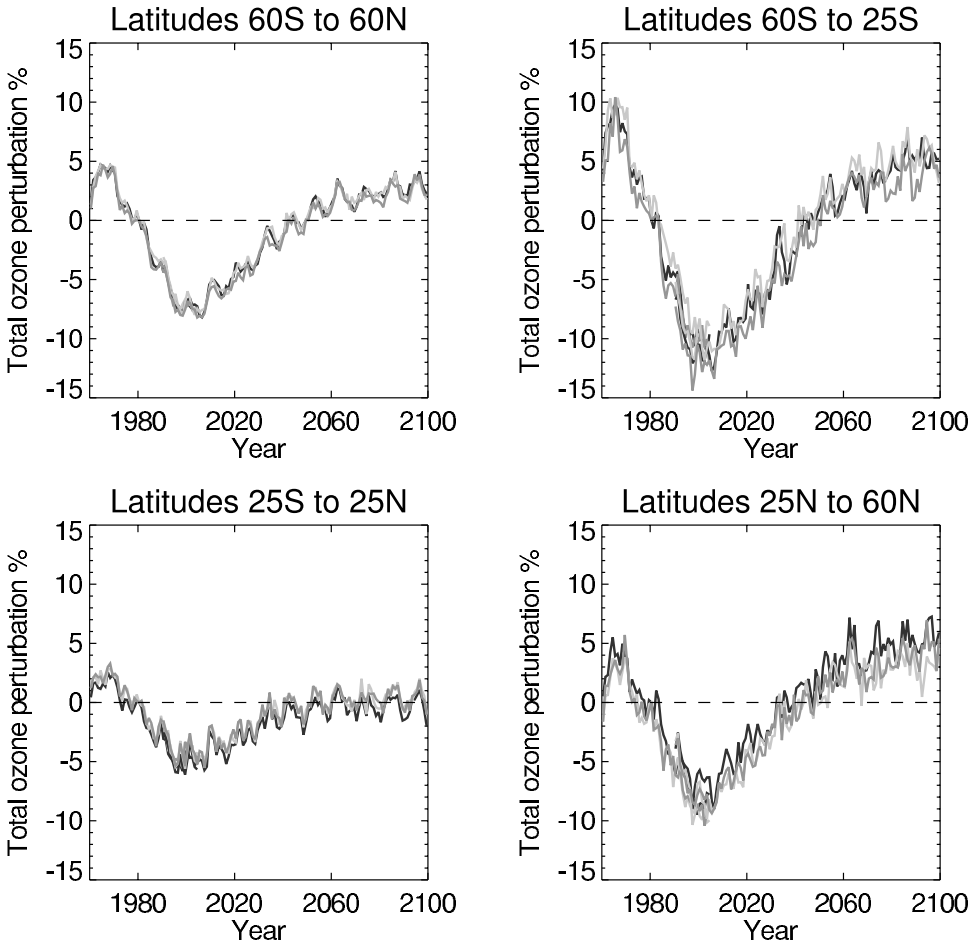

Figure 11. Annually averaged total ozone perturbation for the six transient simulations for selected latitude ranges. Gray scaling is used to denote the different model experiment. The past simulations (1960–2004) and future simulations (1990–2100) have been drawn with the same gray colors, and the 15-year overlap period (1990 to 2004) is drawn for both sets of simulations. The perturbation is relative to the 1980 values.

ments have likely arisen from both improved Cl_y distributions within the vortex and a balance of model errors between vortex temperature and vortex area. For example it is possible to adjust the model nonorographic gravity wave forcing parameters to obtain a larger vortex area in better agreement with observations, but the model lower stratosphere is then colder than observed during winter. With our current model version, it appears not to be possible to get simultaneous agreement with observations for both ozone hole area (or vortex area) and minimum ozone (or vortex temperatures). In the current model version the model wave dynamics are too active, leading to a small polar vortex, a feature that is common to other models (G. Roff, personal communication, 2005).

[31] The annual development of the ozone hole, decade by decade, is illustrated in Figure 14. The results were averaged over the three ensemble members for the whole of each decade indicated and the results were then plotted. The model ozone hole area peaked in the decade 2000–2010 and then decreased further each decade, but a small ozone hole was still present in the 2060s. The broken lines indicate the timing of maximum ozone hole size. The date of the maximum is almost linearly related to the area, with peak depletion drifting from day 266 (23 September, 2000s) to day 278 (5 October, 2050s). The model is in qualitative agreement with observations [e.g., *Bodeker et al.*, 2005] which indicate that the peak ozone hole area occurred on typically day 258 for the 2000s atmosphere and on about day 278 for the incipient ozone hole.

6. Ozone Recovery

[32] Here we consider the "start of ozone recovery" as the time of the minimum value, after smoothing over the 11-year solar cycle. We consider full ozone recovery as "the return of solar cycle-averaged total column ozone to the 1980 values." This was calculated by taking the ratio of the evolving column ozone by the 1980 (solar cycle-smoothed) value, as functions of latitude. For each ensemble member the past simulation up to 1990 (run TRANSA, etc.) has been joined to the future simulation from 1990 onward (run FUTURA, etc.).

[33] The differences between the ensemble members were small and hence only the ensemble mean results are shown (Figure 15). High ozone prior to 1980 is clearly apparent over Antarctica, but otherwise, the past results have no

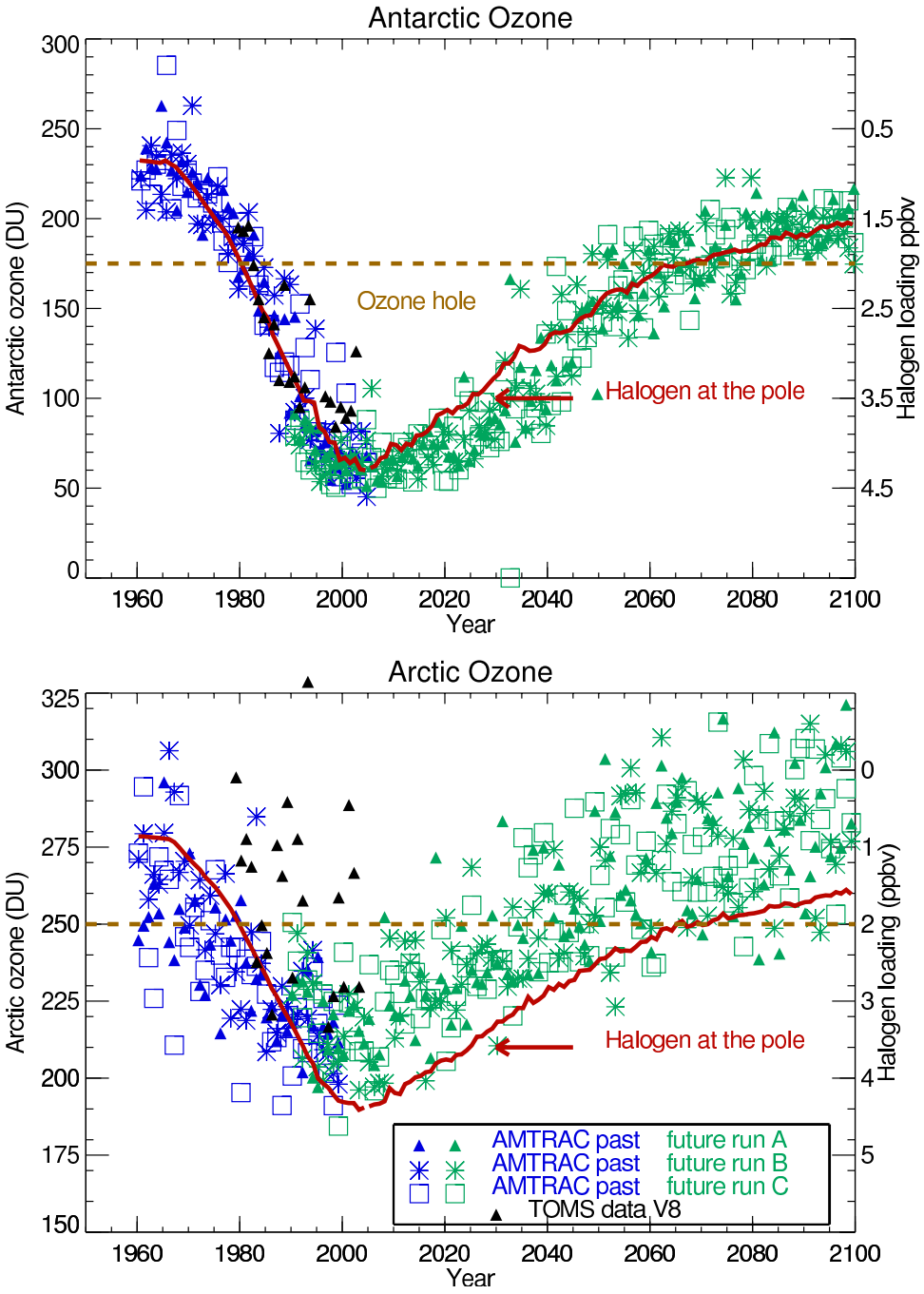

Figure 12. Minimum spring ozone in the model simulations (individual points and left axis) in comparison with TOMS version 8 data for the (top) Antarctic and (bottom) Arctic. The lower stratospheric halogen amount, defined as $Cl_y + 50\times \mathrm{Br}_y$, is also shown for comparison (solid line and right axis scale).

particularly outstanding features. The depletion of ozone over the polar regions is very clear thereafter, with minimum ozone occurring at all latitudes during the period 1998–2005. On this basis, the model simulations imply that ozone recovery should have already begun in the atmosphere, although as noted by *Weatherhead et al.* [2000] more years of observations are required to confirm this point. From the time of the minimum, model ozone recovery occurred monotonicly with each decade. Over Antarctica, 1980 total ozone values were attained by about 2065 on average, the same as the timescale noted earlier for the disappearance of the ozone hole. In contrast, Arctic recovery occurred by 2030 to 2040. Since Antarctic ozone is controlled by the chemistry to a significant degree (Figure 12), the possible implication is that climate change has little impact on the development of the Antarctic ozone hole. In contrast, in the Arctic, the relatively early return to 1980 conditions, suggests that climate change, primarily

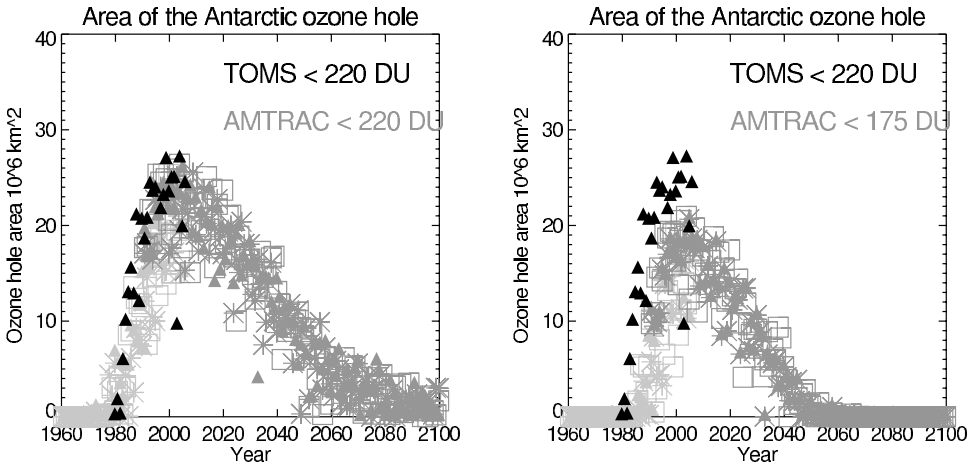

Figure 13. Area of the Antarctic ozone hole in the model simulations in comparison with TOMS V8 data as a function of year. Values have been averaged for the period 21–30 September. (left) Comparisons between TOMS 220 DU areas and AMTRAC 220 DU areas. (right) Comparisons between TOMS 220 DU areas and AMTRAC 175 DU areas.

increases in CO_2 and in particular its impact in strengthening the Brewer-Dobson circulation [*Butchart and Scaife*, 2001], speeds up ozone recovery through increased ozone transport. Clearly, this is just one model and these results need to be interpreted with caution following the demonstrated poor agreement between different models in the Arctic [*Austin et al.*, 2003].

[34] Toward the end of the century, all three model simulations predicted ozone amounts which are substantially higher than simulated for 1980, particularly in the Arctic (Figure 15). This is due to the combined effects of decreased homogeneous ozone destruction from CO_2 cooling and further increased strength of the Brewer-Dobson circulation. There is close consistency between the three ensemble members (not shown). Some of the details, such as the precise location of the 1.0 "full recovery" contour in the tropics, suggest that the forcing data, especially the SSTs, are of prime importance.

[35] The results for each of the four seasons are shown in Figure 16. The solstice seasons are similar to each other and to the annual average, in indicating global ozone loss from 1980 onward, especially in the polar regions. During these seasons, full ozone recovery is also established on the same time frame as in the annual average. However, for the equinox seasons, there are two main differences compared with the annual average relating to the failure of the simulated ozone to return to 1980 values in all latitudes before the year 2095. During northern spring, tropical ozone remained below 1980 levels in a narrow band. This is a small effect and bearing in mind the absence of a Quasi-biennial Oscillation from the model dynamics may not be a reliable result. A possibly larger consequence is the incomplete recovery in spring ozone south of 75°S. The differences in timing between the various diagnostics shown here (Figures 11–15) illustrate potential timing differences in the future real atmosphere. These differences indicate that atmospheric ozone will likely have a different distribution of ozone in the future than in the past, a point made on previous occasions [e.g., *WMO*, 2003, chapter 3]. The very late recovery in Antarctic spring indicated in Figure 16 may also simply be an idiosyncracy of our model, and hence we await confirmation or otherwise from other model simulations.

7. Conclusions and Discussion

[36] Ensemble simulations of a high-resolution coupled chemistry-climate model have been presented for the period 1960 to 2100. The period was split between the past (1960 to 2005) in which each ensemble member was forced with observed data (sea surface temperatures, SSTs; tropospheric and volcanic aerosol, solar cycle and well-mixed greenhouse gases, GHGs), and the "future," covering the period 1990 to 2100. The future runs were forced with model SSTs, background stratospheric aerosol amounts beyond 1997, and the concentrations of the GHGs were taken from the A1B scenario. Results for the 15-year overlap period

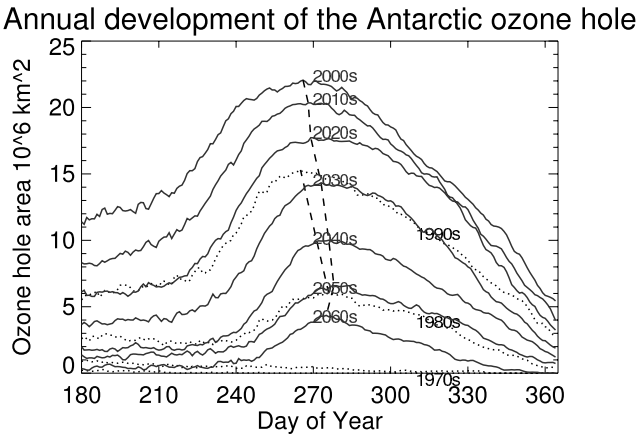

Figure 14. Annual development of the Antarctic ozone hole area in the model by decade, based on the 220 DU total ozone contour. The broken lines indicate the axis of maximum values. The solid lines indicate the results from the ensemble mean of the future runs. The dotted lines indicate the mean of the results for the past runs.

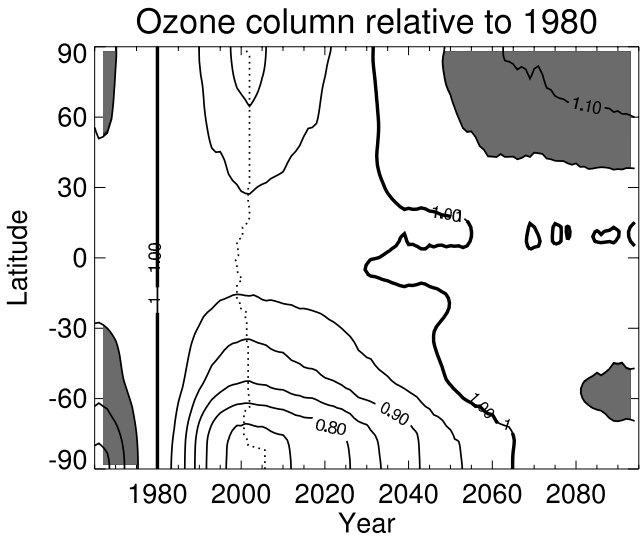

Figure 15. Annual mean total ozone as a function of time divided by the values for the year 1980 for the ensemble mean results. Dashed lines indicate the axis of minimum values, "the start of ozone recovery." The 1.0 contour beyond 1980 indicates "the return to full ozone recovery." Before computing the total ozone ratios, 11-year running means were computed to reduce the impact of the solar cycle. The shaded region indicates values greater than 1.05.

were found to be consistent for most quantities despite differences in SSTs.

[37] The past results were found to be sensitive to the volcanic aerosol present, but this depended on the concentration of chlorine, in accordance with the work of *Tie and Brasseur* [1995]. Ozone increased after the eruption of Agung, but reduced slightly after the eruption of El Chichon and more substantially following the eruption of Mount Pinatubo. Our results for the 1960s differ slightly from those of other recent model simulations [*Dameris et al.*, 2005; C. Brühl, personal communication, 2005] which gave only a slight ozone increase during the Agung eruption. This could be related to the impact of HO_x catalyzed ozone depletion which in our results is smaller due to a more muted radiative effect of the Agung volcanic aerosol itself.

[38] The solar cycle variation in ultraviolet also influenced ozone amounts making it difficult to separate the various factors controlling the global ozone amounts. To allow for these effects, ozone amounts were smoothed over the 11-year solar cycle period. Minimum ozone occurred between 1998 and 2005 depending on ensemble member with no clear latitudinal dependence. Modeled past total ozone decreases since 1980 were almost twice the observed values of about 2–3% per decade outside the polar regions and the overall model ozone was biased low. Nonetheless, the model reproduced many of the observed features of the atmosphere. In particular, the Antarctic ozone hole developed rapidly in the model from about the late 1970s in good agreement with observations and peak depletion occurred by about 2000–2005.

[39] The simulated Antarctic ozone hole did not disappear until about 2065 and a small residual ozone hole was occasionally present up to a decade or more beyond that. During the recovery phase, interannual and ensemble variability of ozone was much larger than for the period of ozone hole formation, making the exact timing of recovery difficult to determine. For reasons partially related to interannual variability, the timing of the disappearance of the ozone hole depends critically on the precise definition adopted. Correcting for the total ozone bias is complex. Assuming the usual ozone hole definition of 220 DU and allowing for a 45 DU bias in our simulations, tests were applied using a 175 DU ozone hole. This gives the most favored recovery date of 2065 specified above. However, taking a 30 DU bias, or 190 DU ozone hole criterion would imply that the model ozone hole would not have disappeared until 2085. Even then, small ozone holes would be predicted until the end of the century.

[40] The definition of an ozone hole as that which occurs when the ozone decreases below 220 DU is an arbitrary one, but instead full recovery can be defined as the return to 1980 ozone values. If the model values are appropriately time-smoothed to eliminate solar effects and interannual variability in the dynamics, the model was found not to recover fully in the Antarctic spring prior to the end of the model simulation. This could be a highly model dependent result, or a highly significant one for the biosphere if it is realized in practice.

[41] In the Arctic, model total ozone recovered to the 1980 column amount by about 2030 for the zonally averaged quantity and about 2040 for the seasonal minimum quantity. By this time interannual variability was also very large, but there was no sign of severe ozone depletion, of Antarctic ozone hole standards, in any of the simulations covering some 195 years for the period 1990–2030. Therefore it is predicted that the lowest ozone has already occurred or will be a small perturbation from the current lowest levels. Again, AMTRAC is just one of many models that is undergoing continual development to obtain improved results. The model intercomparison of *Austin et al.* [2003] showed large differences in the Arctic, and such uncertainties will likely continue. All the same, it is important to note that there is a growing consensus [*Austin et al.*, 2003] that further severe Arctic ozone depletion is unlikely.

[42] On the multidecadal time frame, the impact of climate change is an important issue. In the atmosphere, there will likely be an increase in the strength of the Brewer Dobson circulation [*Butchart and Scaife*, 2001; *Butchart et al.*, 2006]. This will increase the transport of CFCs into the stratosphere so that their atmospheric timescale will be reduced. The increased circulation is not fully taken into consideration by the tropospheric forcing values used in our model simulations and would advance the timing for ozone recovery by about a decade. Ozone recovery itself would respond by partially reducing the change in the Brewer-Dobson circulation [*Austin et al.*, 2006]. A more direct impact of climate change may be deduced by considering the different recovery timescales in the Arctic and Antarctic. The results obtained here suggest that Arctic ozone will recover earlier than Antarctic ozone by some 25 to 35 years. The earlier Arctic recovery is a combined effect of both increased Brewer-Dobson circulation and reduced homogeneous ozone depletion in a cooler stratosphere. These processes affect the Arctic more than the Antarctic because

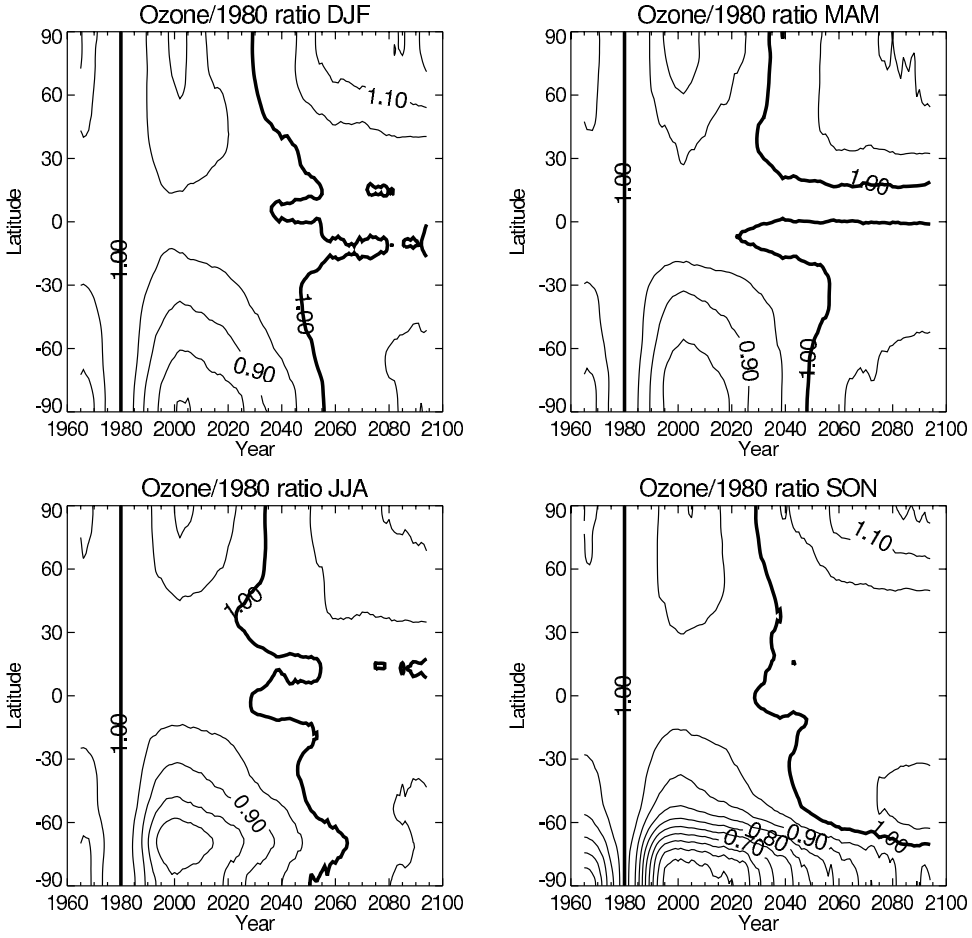

Figure 16. Ensemble mean total ozone for the four seasons as a function of time divided by the values for the year 1980. The bold 1.0 contour beyond 1980 indicates "the return to full ozone recovery." Before computing the total ozone ratios, 11-year running means were computed to reduce the impact of the solar cycle.

the polar vortex is weaker and planetary waves transport more ozone into high latitudes. In comparison, the Antarctic ozone minimum follows closely the evolution of chlorine and bromine amounts, implying that the ozone hole is dominated by chemical changes.

[43] **Acknowledgments.** V. Ramaswamy is thanked for his comments on this work throughout its execution and in stimulating the running of an ensemble of model simulations. Dan Schwarzkopf is thanked for supplying advice on the radiation data sets. Gera Stenchikov provided helpful advice on the volcanic aerosol data sets. Rich Gudgel provided the updated SSTs used in the past simulations. Eugene Rozanov and Hamish Struthers are thanked for discussions during model development. Bill Randel is thanked for supplying data for Figure 6, and Paul Newman kindly supplied TOMS data for Figure 13 ahead of publication. Larry Horowitz and two reviewers provided useful suggestions for improvements to the manuscript. The GFDL computer services personnel provided valuable help throughout the hot summer months to keep the model simulations running. This work would not have been possible without the pioneering efforts of the GFDL Global Atmosphere Model Development Team. J.A.'s research was supported by the Visiting Scientist Program at the NOAA Geophysical Fluid Dynamics Laboratory, administered by the University Corporation for Atmospheric Research.

References

Alexander, M. J., and T. J. Dunkerton (1999), A spectral parameterization of mean flow forcing due to breaking gravity waves, *J. Atmos. Sci.*, *56*, 4167–4182.

Anderson, J. L., et al. (2004), The new GFDL global atmosphere and land model AM2/LM2: Evaluation with prescribed SST simulations, *J. Clim.*, *17*, 4641–4673.

Austin, J. (2002), A three-dimensional coupled chemistry-climate model simulation of past stratospheric trends, *J. Atmos. Sci.*, *59*, 218–232.

Austin, J., and N. Butchart (2003), Coupled chemistry-climate model simulations for the period 1980 to 2020: Ozone depletion and the start of ozone recovery, *Q. J. R. Meteorol. Soc.*, *129*, 3225–3249.

Austin, J., N. Butchart, and K. P. Shine (1992), Possibility of an Arctic ozone hole in a doubled-CO_2 climate, *Nature*, *360*, 221–225.

Austin, J., et al. (2003), Uncertainties and assessments of chemistry-climate models of the stratosphere, *Atmos. Chem. Phys.*, *3*, 1–27.

Austin, J., J. Wilson, F. Li, and H. Voemel (2006), Evolution of water vapor and age of air in coupled chemistry climate model simulations of the stratosphere, *J. Atmos. Sci.*, in press.

Bodeker, G. E., H. Shiona, and H. Eskes (2005), Indicators of Antarctic ozone depletion, *Atmos. Chem. Phys.*, *5*, 2603–2615.

Brasseur, G., and S. Solomon (1987), *Aeronomy of the Middle Atmosphere*, Springer, New York.

Butchart, N., and A. A. Scaife (2001), Removal of chlorofluorocarbons by increased mass exchange between the stratosphere and the troposphere in a changing climate, *Nature*, *410*, 799–802.

Butchart, N., et al. (2006), A multi-model study of climate change in the Brewer-Dobson circulation, *Clim. Dyn.*, in press.

Dameris, M., et al. (2005), Long-term changes and variability in a transient simulation with a chemistry-climate model employing realistic forcing, *Atmos. Chem. Phys.*, *5*, 2121–2145.

Delworth, T. L., et al. (2006), GFDL's CM2 global coupled climate models - Part 1: Formulation and simulation characteristics, *J. Clim.*, *19*, 643–674.

Fioletov, V. E., G. E. Bodeker, A. J. Miller, R. D. McPeters, and R. Stolarski (2002), Global and zonal total ozone variations estimated from ground-based and satellite measurements: 1964–2000, *J. Geophys. Res.*, *107*(D22), 4647, doi:10.1029/2001JD001350.

Groves, K. S., and A. F. Tuck (1980), Stratospheric O_3-CO_2 coupling in a photochemical-radiative column model. II With chlorine chemistry, *Q. J. R. Meteorol. Soc.*, *106*, 141–157.

Intergovernmental Panel on Climate Change (IPCC) (2001), *Climate Change 2001: The Scientific Basis. Third Assessment Report*, edited by Houghton, J. T., et al., Cambridge Univ. Press, New York.

Knutson, T. R., T. L. Delworth, K. W. Dixon, I. M. Held, J. Lu, V. Ramaswamy, M. D. Schwarzkopf, G. Stenchikov, and R. J. Stouffer (2006), Assessment of twentieth-century regional surface temperature trends using the GFDL CM2 coupled models, *J. Clim.*, *19*, 1624–1651.

Labitzke, K., J. Austin, N. Butchart, J. Knight, J. Haigh, and V. Williams (2002), The global signal of the 11-year solar cycle in the stratosphere: Observations and model results, *J. Atmos. Sol. Terr. Phys.*, *64*, 203–210.

Miller, A. J., A. Cai, G. Tiao, and D. Wuebbles (2006), Examination of ozonesonde data for trends and trend changes including solar and arctic oscillation signals, *J. Geophys. Res.*, *111*, D13305, doi:10.1029/2005JD006684.

Newchurch, M. J., E. S. Yang, D. M. Cunnold, C. C. Reinsel, J. M. Zawodny, and J. M. Russell III (2003), Evidence for slowdown in stratospheric ozone loss: First stage of ozone recovery, *J. Geophys. Res.*, *108*(D16), 4507, doi:10.1029/2003JD003471.

Newman, P. A., E. R. Nash, S. R. Kawa, S. A. Montzka, and S. M. Schauffler (2006), When will the Antarctic Ozone hole recover?, *Geophys. Res. Lett.*, *33*, L12814, doi:10.1029/2005GL025232.

Randel, W. J., F. Wu, S. J. Oltmans, K. Rosenlof, and G. E. Nedoluha (2004), Interannual changes of stratospheric water vapor and correlations with tropical tropopause temperatures, *J. Atmos. Sci.*, *61*, 2133–2148.

Reinsel, G. C., A. J. Miller, E. C. Weatherhead, L. E. Flynn, R. M. Nagatani, G. C. Tiao, and D. J. Wuebbles (2005), Trend analysis of total ozone data for turnaround and dynamical contributions, *J. Geophys. Res.*, *110*, D16306, doi:10.1029/2004JD004662.

Sander, S. P., et al. (2003), Chemical kinetics and photochemical data for use in atmospheric studies, Evaluation Number 14, *JPL Publ., 02-25*.

Shindell, D., D. Rind, N. Balachandran, J. Lean, and P. Lonergan (1999), Solar cycle variability, ozone and climate, *Science*, *284*, 305–308.

Solomon, S., R. W. Portmann, T. Sasaki, D. J. Hofmann, and D. W. J. Thompson (2005), Four decades of ozonesonde measurements over Antarctica, *J. Geophys. Res.*, *110*, D21311, doi:10.1029/2005JD005917.

Steinbrecht, W., H. Claude, and P. Winkler (2004), Enhanced upper stratospheric ozone: Sign of recovery or solar cycle effect?, *J. Geophys. Res.*, *109*, D02308, doi:10.1029/2003JD004284.

Steinbrecht, W., et al. (2006), Long-term evolution of upper stratospheric ozone at selected stations of the Network for the Detection of Stratospheric Change (NDSC), *J. Geophys. Res.*, *111*, D10308, doi:10.1029/2005JD006454.

Tie, X., and G. Brasseur (1995), The response of stratospheric ozone to volcanic eruptions: Sensitivity to atmospheric chlorine loading, *Geophys. Res. Lett.*, *22*, 3035–3038.

Weatherhead, E. C., et al. (2000), Detecting the recovery of total column ozone, *J. Geophys. Res.*, *105*, 22,201–22,210.

Wellemeyer, C. G., P. K. Bhartia, R. D. McPeters, S. L. Taylor, and C. Ahn (2004), A new release of data from the Total Ozone Mapping Spectrometer (TOMS), *SPARC Newsl. 22*, pp. 37–38, SPARC Off., Serv. d'Aéron., Verrières-le-Buisson, France.

World Meteorological Organization (WMO)/United Nations Environment Programme (UNEP) (2003), *Scientific Assessment of Ozone Depletion: 2002*, *Rep. 47*, Global Ozone Res. and Monit. Proj., Geneva, Switzerland.

Yang, E. S., M. Newchurch, D. Cunnold, R. J. Salawitch, M. P. McCormick, J. M. Russell III, J. Zadodny, and S. Oltmans (2006), Attribution of recovery in lower stratospheric ozone, *J. Geophys. Res.*, doi:10.1029/2005JD006371, in press.

J. Austin and R. J. Wilson, Geophysical Fluid Dynamics Laboratory, Princeton, NJ 08542-0308, USA. (john.austin@noaa.gov)